MDPI

Article

From Flanders to Portugal: A Portuguese Painter in Pursuit of Prestigious Flemish Painting—Materials and Techniques Compared Through an Analytical Approach

Vanessa Antunes [1,2,*], António Candeias [1,3], José Mirão [3], Sara Valadas [3], Ana Cardoso [1], Maria José Francisco [4], Alexandra Lauw [5], Marta Manso [6,7,8] and Maria Luísa Carvalho [7]

[1] Laboratório José de Figueiredo, Museus e Monumentos de Portugal, EPE (LJF-MMP, EPE), Janelas Verdes s/n, 1200-690 Lisboa, Portugal; candeias@uevora.pt (A.C.); ana.cardoso@museusemonumentos.pt (A.C.)
[2] ARTIS-Instituto História da Arte, Faculdade de Letras, Universidade de Lisboa (ARTIS-IHA/FLUL), Alameda da Universidade, 1600-214 Lisboa, Portugal
[3] Laboratório HERCULES, Escola de Ciências e Tecnologia, Universidade de Évora, Largo Marquês de Marialva 8, 7000-676 Évora, Portugal; jmirao@uevora.pt (J.M.); svaladas@uevora.pt (S.V.)
[4] Museu de Setúbal, Balneário Dr. Paula Borba, 2900-120 Setúbal, Portugal; mjfrancisco5@gmail.com
[5] Centro de Estudos Florestais, Instituto Superior de Agronomia, Tapada da Ajuda, 1349-017 Lisboa, Portugal; alexandra.lauw@gmail.com
[6] Faculdade de Belas-Artes, Universidade de Lisboa, Largo da Academia Nacional de Belas-Artes, 1249-058 Lisboa, Portugal; marta.manso@fct.unl.pt
[7] LIBPhys-UNL, Laboratório de Instrumentação, Engenharia Biomédica e Física da Radiação, Departamento de Física, Faculdade de Ciências e Tecnologia, Universidade Nova de Lisboa, 2829-516 Caparica, Portugal; luisa.carvalho@fct.unl.pt
[8] VICARTE, Vidro e Cerâmica para as Artes, Departamento de Conservação e Restauro, Faculdade de Ciências e Tecnologia, Universidade Nova de Lisboa, 2829-516 Caparica, Portugal
[*] Correspondence: vanessa.antunes@museusemonumentos.pt; Tel.: +351-217-920-000

Abstract: This study offers fresh insights into the technical and stylistic exchanges between Flemish and Portuguese panel painting during the late 15th and early 16th centuries. By comparing two contemporaneous works, we trace Flemish influence in Portugal through a detailed materials and techniques analysis. Non-invasive, in situ methods—including energy dispersive X-ray fluorescence (XRF), macro-photography (MP), infrared reflectography (IRR), and dendrochronology—were used to examine each painting's wooden support, ground layer, underdrawing, and pigment stratigraphy. Select micro-sampling analyses—micro-Fourier-transform infrared spectroscopy (μ-FTIR), scanning electron microscopy with energy dispersive spectroscopy (SEM-EDS), and micro-Raman spectroscopy (μ-Raman)—provided complementary data on binder and pigment composition. While both paintings share nearly identical pigments and layering sequences and employ comparable coating techniques, their ground compositions differ subtly. Notably, the Flemish work features extensive gold-leaf application, whereas underdrawing execution takes on principal importance in the Portuguese example. Together, these findings reveal that Jorge Afonso's workshop developed a distinct Portuguese method—rooted in Flemish practices disseminated by Quentin Metsys—yet adapted to local materials and aesthetic priorities.

Keywords: painting technique; drawing; Flemish painting; Portuguese painting; analytical techniques

1. Introduction

This study concerns the materials and the techniques employed by two masters in their Flemish and Portuguese paintings. Both works depict the same rare theme—the Apparition

of the Angel to Santa Clara, Santa Inês, and Santa Coleta. The Flemish painting (P1), attributed to the workshop of Quentin Metsys (1466–1530) [1], was made circa 1491–1507. It was commissioned by Emperor Maximilian and later offered to Queen D. Leonor of Portugal [1–7]. The Queen likely offered the painting to Convento de Jesús in Setúbal, Portugal. The nuns from this convent would have commissioned a painting on the same theme from Jorge Afonso (c. 1470–1540), the greatest painter of the Lisbon workshop (1517-19/1530). This altarpiece, considered his last and most significant work, was regarded as one of the most important pieces of the 14-painting altarpiece [8–16].

In the past, research on these paintings has been focused on Art History, specifically addressing Jorge Afonso's workshop [16–18] and, more recently, Setúbal altarpiece materials [19].

The iconographic influences of both P1 and P2 are based on northern European models, as seen in an engraving by Martin Schongauer (c. 1470–1480), representing "The Angel of the Annunciation" or in an angel image of Albrecht Dürer engraving, ca. 1510, part of "The Annunciation, from "The Small Passion" (Figure 1).

Figure 1. (**a**) Painting "Apparition of the angel to Santa Clara, Santa Inês and Santa Coleta" (P1), attributed to Quentin Metsys workshop, c. 1491–1507, oil on Baltic oak wood, 1527 × 973 mm, Setúbal museum, Convento de Jesus; (**b**) Albrecht Dürer engraving, ca. 1510, part of "The Annunciation, from "The Small Passion" (reversed detail). The Metropolitan Museum of Art, New York, Gift of Junius Spencer Morgan, 1919, inv.19.73.173; (**c**) Painting "Apparition of the angel to Santa Clara, Santa Inês and Santa Coleta" (P2), the altarpiece of the church of Convento de Jesus in Setúbal, Jorge Afonso, Portuguese school, 1525, oil on Baltic oak wood, 1755 × 1110 mm, Setúbal Museum, Convento de Jesús in Setúbal.

Moreover, art historians claim that P1 might have been the source for P2 [16–18]. However, it remains unclear whether the Portuguese painter Jorge Afonso was influenced by Flemish techniques or if he adhered to Portuguese traditions in terms of materials and techniques.

In the present work, we compare the materials, and the techniques used in P1 and P2 to identify their differences and similarities. Pigments were identified by combining in situ

X-ray fluorescence spectroscopy with ex situ scanning electron microscopy with energy-dispersive spectroscopy and μ-Raman spectroscopy. This analytical methodology provided the stratigraphic characterization of the chemical composition by color and layer [19–26].

The supporting materials and dendrochronology of P1 were examined, since the dendrochronological study of P2 was conducted and subsequently published by Antunes et al. [27].

The novelty of this study lies in presenting, for the first time through analytical results, strong evidence of Flemish influences (P1) on Portuguese painting (P2) since no prior technical or material comparison has been conducted between the two paintings.

2. Materials and Methods

Sample collection and preparation were carried out by embedding samples in an Epofix organic compound with a hardener. Samples were micro-meshed with abrasive cloths in consecutive finer grades.

Observations by optical microscopy (OM) of the cross-sections allowed us to define ground and painting layer numbers. They were performed on a Leica DM 2500M, Leica Microsystems, Wetzlar, Germany optical dark 100-field magnifier coupled to a photographic camera Leica MC170HD, Leica Microsystems, Wetzlar, Germany. Pictures were taken at different magnifications, from $100\times$ to $500\times$.

Macro-photographs (MP) were captured with a mobile microscope 3" LCD 8. 5 Mega Pixels $20–500\times$, Digital LCD with VGA, micro-SD card storage, and a MicroCapture professional software system, Max-see, Taichung, Taiwan. Infrared reflectography (IRR) was performed with a high-resolution infrared reflectography camera (Osiris) with an InGaAs detector, Opus Instruments, Makers of the Apollo & Osiris Infrared Reflectography cameras used in art conservation and research around the world Photography Norwich, Norfolk. It permits a wavelength response from 900 to 1700 nm and is equipped with a 16×16 tile system. This instrument allows a picture size of 4096×4096 pixels. The camera is provided with the long-pass filter Schott RG850, Opus Instruments, Norwich, Norfolk. The infrared wavelength is transmitted, with shorter wavelengths below 850 nm blocked. The reflectograms captured a 60 cm $\times$ 60 cm area and were recorded at an operating distance of 125 cm, considering the front of the body camera to the painting, and focus (front of the body camera to the lens) of 28 cm, with an f/11 aperture. Diffuse illumination at 1000 lux was provided by reflectors with 2×1000 W halogen VC—1000Q Quartz light tone, Opus Instruments, Norwich, Norfolk. The ultimate image, composed of many reflectograms, was assembled in Photoshop CS5 with the Photomerge tool. All the photographs had minimal treatment, adjusting levels, and increased distinction.

The portable X-ray fluorescence spectrometer used in this work permitted the identification of elemental composition by color. It consists of an Amptek Mini-X X-ray tube (Rh, 50 kV, 200 μA, 4 W max) and an Amptek SDD detector with an energy resolution of 140 eV FWHM at 5.9 keV, a 25 mm^2 detection area, and 500 μm thickness [20]. The detector and the X-ray tube are assembled in a 90 geometry. This geometry allows for a high background reduction due to Compton scattering [21]. Analyses were performed in air at 30 kV and 15 μA for 120 s. A 1 mm collimator was used at the exit of the X-ray tube. The spectra were acquired using DppPMCA 1.0.0.22 setup software. Spectra deconvolution and assessment were performed using the version 4.5, Win Axil X-Ray Analysis Software, Canberra Eurisys Benelux, Belgium. Analyses were carried out in situ before sample collection in the same region.

Scanning electron microscopy with energy-dispersive spectrometry (SEM-EDS) provides elemental distribution maps and morphological characterization of the painting materials. The elemental distribution through the cross-sections was performed in backscat-

tering mode with a Hitachi S-3700N SEM coupled with a Bruker XFlash 5010 SDD energy-dispersive detector, Bruker Corporation, Billerica, MA, USA. A variable pressure mode at 40 Pa without carbon coating was performed to allow further analyses. The operating conditions for EDS analysis were 20 kV accelerating voltage and 10 mm working distance.

Micro-Raman spectroscopy analysis (μ-Raman) allowed the confirmation of some inorganic compounds. A Horiba-Jobin Yvon XploRA spectrometer with an air-cooled CCD Andor iDus detector was used, Oxford Instruments plc, Tubney Woods, Abingdon, Oxon OX13 5QX, UK. Spectra were acquired using a 785 nm laser, a 100× magnification objective, a pinhole of 300 μm, an entrance slit of 100 μm, and a 1200 lines/mm diffraction grating in a range of 100–3000 cm^{-1}. A maximum incident power of 0.2 mW was used. Spectra deconvolution was performed using LabSpec (V5.78), PANalytical, Almelo, The Netherlands. Pigment classification was made with Spectral IDTM and alternative databases [22–24].

Binders in the ground and pigment layers were initially identified by micro-Fourier-transform infrared spectroscopy (μ-FTIR) analysis performed using a Bruker spectrometer Tensor 27 model in transmission mode, Bruker Corporation, Billerica, MA, USA. A 15× objective and a diamond compression microcell EXPress 1.6 mm, STJ-0169, at the medium infrared region (MIR) were used. The spectrometer is coupled with a Hyperion 3000 microscope, controlled by software OPUS 7.2 from Bruker, and a Mercury Cadmium Telluride detector, Bruker Corporation, Billerica, MA, USA. A working range of 4000–600 cm^{-1} in a spectral resolution of 4 cm^{-1} and 64 scans/spectrum was recorded.

To undertake a dendrochronological study of the painting, it is first necessary to remove the frame so that the cross-sections of each plank may be analyzed. Subsequent measurements and analyses are then conducted on macro-photographs captured using a camera. Image and statistical treatments were performed in the software system packages Image Analysis (Analysis 2.1), TRICYCLE, Amersfoort, The Netherlands [25], and TSAPWin Scientific 4.64 [26].

3. Results and Discussion

3.1. Supports

Both panels were prepared on four vertically assembled planks of Baltic oak wood. The careful choice of planks is clear in both cases, with radial or full radial cuts chosen to minimize wood shrinkage and its associated problems. The widths of the planks in paintings P1 and P2 range from 22 to 27 cm and from 25 to 31 cm, respectively. Cross-sectional analysis confirmed the absence of sapwood rings in both assemblies.

Dendrochronological study of P1's planks established 1480 as the date of the most recent tree-ring. To establish a terminus post quem for the panel, one must account for both the removed sapwood and the wood's seasoning interval. Based on regional oak characteristics, sapwood removal likely encompassed at least nine rings, and a minimum drying period of two years must be assumed [27–31]. Thus, the panel could not have been painted before 1491 (1480 + 9 + 2). If one adopts the average sapwood ring count of fifteen [31], the implied earliest execution date becomes 1497 (1480 + 15 + 2). However, these calculations do not consider the possible loss of heartwood rings nor any extended seasoning or storage beyond the assumed minimum. In any case, these dates align closely with the generally accepted attribution range for Quentin Metsys's painting (c. 1491–1507). For P2, the "presumed date of use" has been determined as 1508 [27], coinciding with the year Jorge Afonso's appointment as royal painter by King D. Manuel I of Portugal. A penciled inscription on the verso reads "525", which—interpreted in the context of the panel's chronology—falls four years before Metsys's death [27]. This apparent discrepancy likely reflects variations in seasoning times, storage intervals, and sapwood removal during assembly.

Together, these findings underscore the political and artistic importance of Metsys's Setúbal workshop (P1) and provide the context for commissioning Jorge Afonso's corresponding panel (P2), both conceived within the same thematic program and eventually integrated into the larger altarpiece.

3.2. Ground Layers

A comparison of the two panels reveals marked differences in their craquelure patterns. In P1, the ground layer is thin and highly fractured, comprising at least three coats of chalk—each finer than the last—and the final coat aligned with the wood's radial grain. This chalk, rich in calcite ($CaCO_3$) (Table 1), provides an ideal, light-reflective texture for oil paint and was a hallmark of Northern European masters [28–32]. Cross-section measurements show a progressive reduction in thickness from the bottom to the top coats (48 μm, 18 μm, and 11 μm, respectively) (Figure 2a,b). SEM backscattered electron imaging of sample P1-33 reveals coccolith and foraminifera fossils, confirming the use of natural chalk, and EDS mapping identifies calcium as the principal element in the ground matrix (Figure 2d).
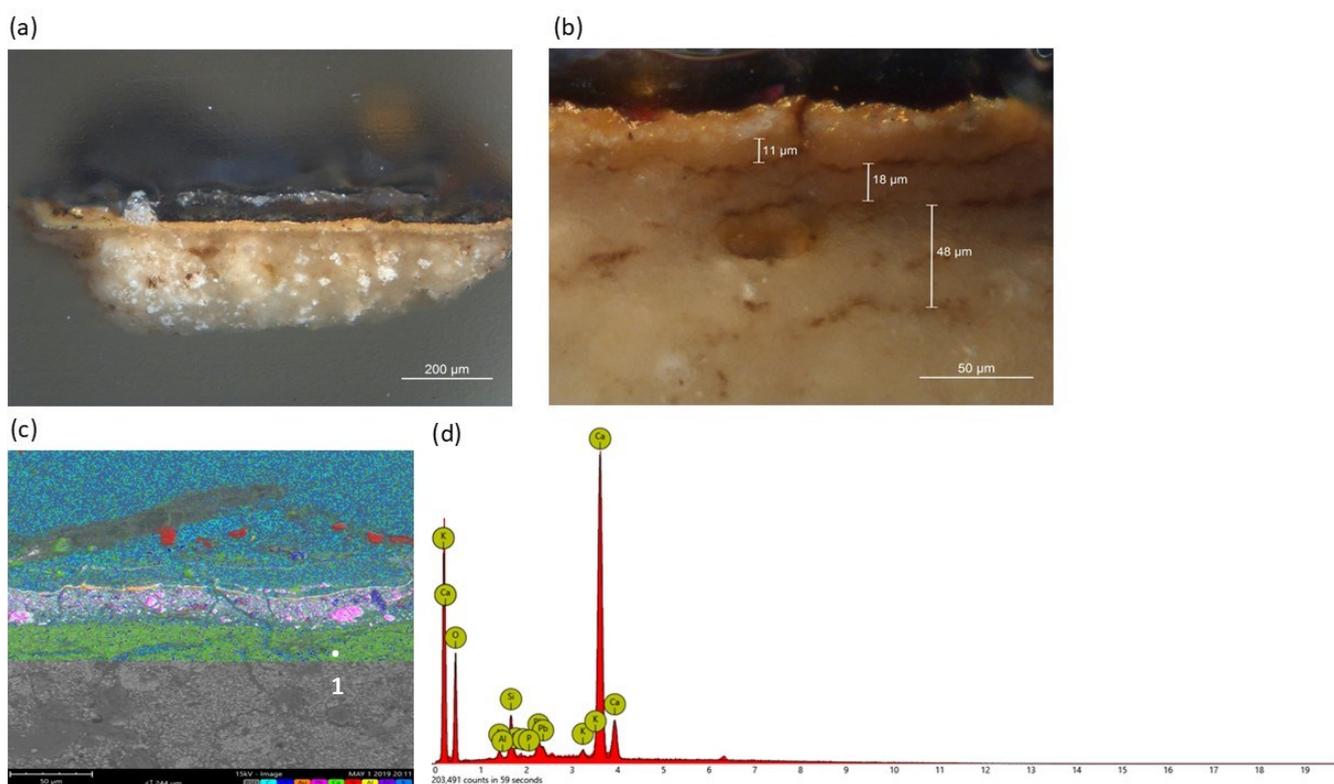

Figure 2. (**a**) OM image of a sample taken from the golden light tone from the angel's wing (P1-7); (**b**) OM detail of the same sample highlighting the decrease in thickness from bottom to upper coats (48 μm, 18 μm, 11 μm) of the ground layer; (**c**) SEM-EDS distribution of the chemical elements present in P1-7, highlighting Ca matrix in the ground -layer and the presence of Pb, Al, and Si in the bol layer; (**d**) EDS spectrum of the same sample, highlighting the presence of Ca as a main element of ground layer matrix.

Micro-FTIR analysis of the uppermost layer (sample P1-7) detected calcite, trace amounts of gypsum and cerussite, silicates, and protein; the first ground coat likewise contained calcite, gypsum, silicates, and protein (Table 2). The sulfate bands observed may also result from the garlic used in the sizing layer, as previously noted [33].

Table 1. Main pigments by color of the P1 accessed using the μ-Raman technique.

Sample	Color/Area	Micro-Raman Key Compounds (cm^{-1})
P1-1	white light tunic angel	ground layer: calcite (286, 1091); white layer: plumbonacrite (324, 414, 1055), hematite (228, 293, 409, 500, 613);
P1-2	white angel tunic shadow	red layer: hematite (226, 294, 412, 504, 618); black layer: azurite (213, 250, 404, 771, 832, 939, 1099)
P1-3	yellow light custody	yellow layer: lead-tin yellow type I (132, 160, 309, 415, 460), carbon black (1321, 1557)
P1-6	ochre background shadow	brown layer: carbon black (1331, 1577), hematite (230, 297, 415), lead-tin yellow type I (130, 197, 266)
P1-7	golden light angel wing	white layer: lead white (1060); bol layer: vermilion (255, 271), gold; black layer: carbon black (1336, 1585),
P1-10	black wing angel	black layer: Carbon black (1361, 1616)
P1-12	red shadow column	red layer: hematite (228, 247, 296, 413, 491, 611), carbon black (1346, 1600)
P1-13	red mantle of the apostle in the background	white layer: lead white (1054), carbon black (1343, 1603); red layer: vermilion (254, 287, 344),
P1-14	golden nimbus Sta. Clara	white layer: lead white (1054), carbon black (1325, 1608);
P1-15	light brown tunic Sta.Clara	yellow layer: lead white (1056), hematite (225, 247, 291, 405, 413, 538), carbon black (1323, 1600)
P1-17	light brown architecture	brown layer: lead-tin yellow type I (130, 199, 278, 293, 460, 530), lead white (1053), carbon black (1337, 1588)
P1-20	brown angel hair shadow	brown layer: carbon black (1352, 1577), cinnabar (254, 294, 345), hematite (230, 297, 415); White layer: lead white (1055)
P1-21	light green ground	green layer: lead-tin yellow type I (130, 159, 196, 277, 296, 459, 527), hematite (225, 292, 413, 599), carbon black (1301, 1549)
P1-22	green shadow floor	carbon black (1340, 1581), goethite (258, 304, 385, 477, 547)
P1-23	green light trees	blue layer: azurite (236, 280, 324, 399, 631, 763, 832, 1015, 1095), cerusite (258, 1058); green layer: plumbonacrite (130, 194, 276, 463), lead tin yellow tipe I (129, 151, 196, 268, 453), malachite (267, 352, 397, 435, 536, 612, 726, 768, 868, 939, 1007, 1095),
P1-24	green shadowtrees	blue layer: azurite (278, 332, 372, 401, 593, 766, 832, 911, 1093), cerusite (213, 1056), hematite (225, 292, 413, 494, 614),
P1-26	blue sky shadow	blue layer: azurite (280, 401, 536, 777, 831, 1097), barite (461, 618, 648, 989), plumbonacrite (316, 401, 1058), carbon black (1335, 1575);
P1-28	gray shadow tower	yellow layer: lead tin yellow type I (130, 158, 196, 266, 456); gray layer: carbon black (1342, 1578), lead white (1052), azurite (249, 284, 394, 766, 811, 940, 1099);
P1-30	black shadow veil Sta.Clara	yellow layer: lead tin yellow type I (131, 160, 196, 0276, 459), lead white (1051), carbon black (1320, 1581); black layer: carbon black (1326, 1583), red ochre (219, 285, 398, 487, 595)
P1-31	carnation light hand Sta.Clara	carnation: lead-tin yellow type II (135, 216, 278, 393), lead white (1058)
P1-32	hand shadow Sta.Clara	carnation: carbon black (1344, 1571), lead white (1055)
P1-34	shadow angel hand	carnation: carbon black (1327, 1597), lead white (1055), hematite (225, 248, 412, 501, 610), cinnabar (255, 289, 343),
P1-36	golden shadow crown	bol layer: lead tin yellow type I (128, 194, 273, 288, 453), plumbonacrite (292, 402, 1054), calcite (292, 720, 1091), hematite (222, 247, 291, 409, 494, 613), cinnabar (254, 285, 341), carbon black (1303, 1607)

Table 2. Micro-FTIR results for P1 and P2.

Sample	Layer	Micro-FTIR Compounds (cm^{-1})
P1-2	blue	Azurite (3429, 1091, 956, 839, 815, 770, 742), Cerussite (1418, 1051, 681), Oil (2926, 2852, 1705), Lead carboxylates (1539)
P1-7	varnish	Ketone resin (2923, 2852, 1706, 1448)
	bolus	Kaolinite (3698, 914), Cerussite (1051), Hydrocerussite (1045, 839, 679), Calcite (2517, 1415, 876, 712), traces of Gypsum (1621, 1108, 1005, 609), Quartz (1080, 796, 780), Ketone resin (2922, 2853, 1704, 1447), Oil (1100), Lead carboxylates (1549), Oxalates (1322)
	upper ground layer	Calcite (2512, 1796, 1435, 876, 713), traces of Gypsum (3409, 1619, 1112, 673, 608), traces of Hydrocerussite (1045, 839, 677), Silicates (780), Protein (2920, 2850, 1646)
	inferior ground layer	Calcite (2512, 1796, 1415, 875, 712), Gypsum (3402, 1620, 1119, 673), Silicates (782), Protein (2921, 2851, 1645)
P1-9	red lacquer	Hydrocerussite (1043, 839, 678), Calcite (1417, 876, 712), Gypsum (3406, 1681, 1621, 1111, 671), Silicates (779), Ketone resin (2924, 2851, 1448)
P1-14	bolus	Kaolinite (3699, 3619, 914), Cerussite (1051), Hydrocerussite (3535, 1046, 839, 681), Calcite (2516, 1793, 1419, 875, 712), traces of Gypsum (3408, 1618), Oil (1726, 1100, 724), Protein (2928, 2852, 1646, 1552), Ketone resin (1709, 1447), Metal carboxylates (1529), Oxalates (1323, 780)
P2-2	blue	Azurite (3428, 1091, 954, 838, 815, 770, 741), Cerussite (1052, 687), Ketone resin (2923, 2851, 1709, 1446), Metal carboxylates (1511)
P2-14	bolus	Kaolinite (3699, 3650, 3620, 1034, 1010, 914), Cerussite (1050), Hydrocerussite (3527, 1409, 1045, 838, 680), Quartz (796, 780), Oil (2920, 2851, 1725, 1102, 721), Lead carboxylates (1519)
	ground layer	Gypsum (3536, 3485, 3405, 3248, 1621, 1118, 673), Anhydrite (1015, 614), Protein (2930, 2856, 1646, 1558), Carbonate (1407)
P2-30	black	Cerussite (1406, 1051, 839, 679), Quartz (1084, 797, 780), Gypsum (3400, 1619), Ketone resin (1448, 727), Oil (2927, 2853, 1707, 1164, 722), Metal carboxylates (1545)
P2-32	black	Cerussite (1051, 839, 679), Gypsum (3404, 1623, 1121, 673), Quartz (1084, 797, 780), Wax (730, 719), Ketone resin (2924, 2851, 1707, 1447), Oil (1102), Lead carboxylates (1520)

By contrast, P2 exhibits a thicker, less regular craquelure, typical of a two-stage calcium sulfate ground. A coarser-grained lower layer is overlaid by a finer upper layer of the same material. This $CaSO_4$ system, characteristic of Portuguese panel painting and part of the Southern European tradition, has been documented in prior studies [34–36] and among followers in Jorge Afonso's workshop [37–39].

One reason Jorge Afonso's workshop employed calcium sulfate grounds is that natural chalk was not locally available in Portugal. During this period, Portugal faced political and economic challenges, including the decline of its Antwerp "feitoria", [1] which likely disrupted the import of "giz de pintores" (painters' chalk). Consequently, calcium carbonate is almost entirely absent in the ground layers studied from Jorge Afonso's workshop. Nevertheless, micro-FTIR analysis of the upper, thinner ground layer (sample P2-14) detected minor amounts of calcite—probably added to smooth the anhydrite matrix and produce a finer surface for drawing and painting. This small admixture of carbonate may reflect a local adaptation of Flemish techniques and materials to Portuguese conditions [34,35,40,41]. The same analysis also confirmed the presence of gypsum, anhydrite, proteinaceous binder, and carbonate bands at 1407 cm^{-1} (Table 2).

3.3. Drawing and Priming Layers

The underdrawings of P1 and P2 differ markedly. In P1, the underdrawing is scarcely detectable by infrared reflectography (Figure 3). This may indicate either the omission of a traditional carbon sketch—perhaps a consequence of high-volume production in a Flemish workshop using pattern-transfer techniques (cartoons or pouncing)—or the employment of non-carbon media, such as metalpoint. Apprentices often executed their initial studies in metalpoint or leadpoint on smooth, chalk-prepared grounds during their first year of training, before progressing to pen or brush work. These metalpoint techniques, inherited from manuscript illumination practices, are ideally suited to finely ground chalk surfaces [42,43].
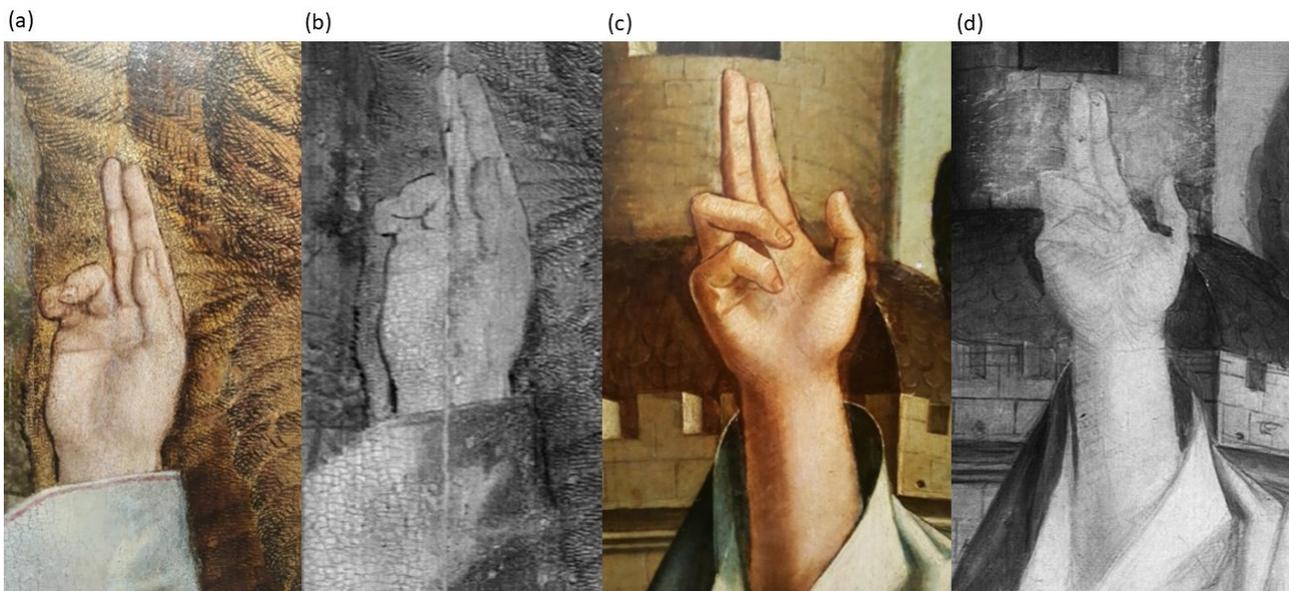
Figure 3. (**a**) Painting "Apparition of the angel to Santa Clara, Santa Inês and Santa Coleta" (detail), attributed to Quentin Metsys workshop, c. 1491–1507; (**b**) reflectogram of the same detail showing scarce underdrawings; (**c**) painting "Apparition of the angel to Santa Clara, Santa Inês and Santa Coleta" (detail), the altarpiece of the church of the Convento de Jesus, Setúbal, Jorge Afonso, Portuguese school, 1525; (**d**) reflectogram of the same detail showing shadow marking and fingers correction underdrawings.

The metalpoint technique gained prominence among Flemish and Italian artists in the early Renaissance, as documented by Cennini in his late 14th-century treatise [44,45]. Silverpoint styluses varied in alloy composition from pure silver to copper-containing mixtures [46]. Leadpoint was likewise used, though its presence is difficult to detect by infrared reflectography or radiography because of the lead-white priming layer [47,48], which is found on both P1 and P2. In P2, leadpoint may indeed have contributed to the underdrawing: optical microscopy of sample P2-39 revealed an indistinct layer containing red grains that EDS identified as lead—most likely minium—supporting the use of leadpoint on that panel (Figure 4).

Unlike P1, the underdrawing in P2 combines both dry leadpoint sketching and carbon-based media [27]. It reveals a careful delineation of figure contours and shadow modeling, with evidence of preliminary—or "abandoned"—sketches.
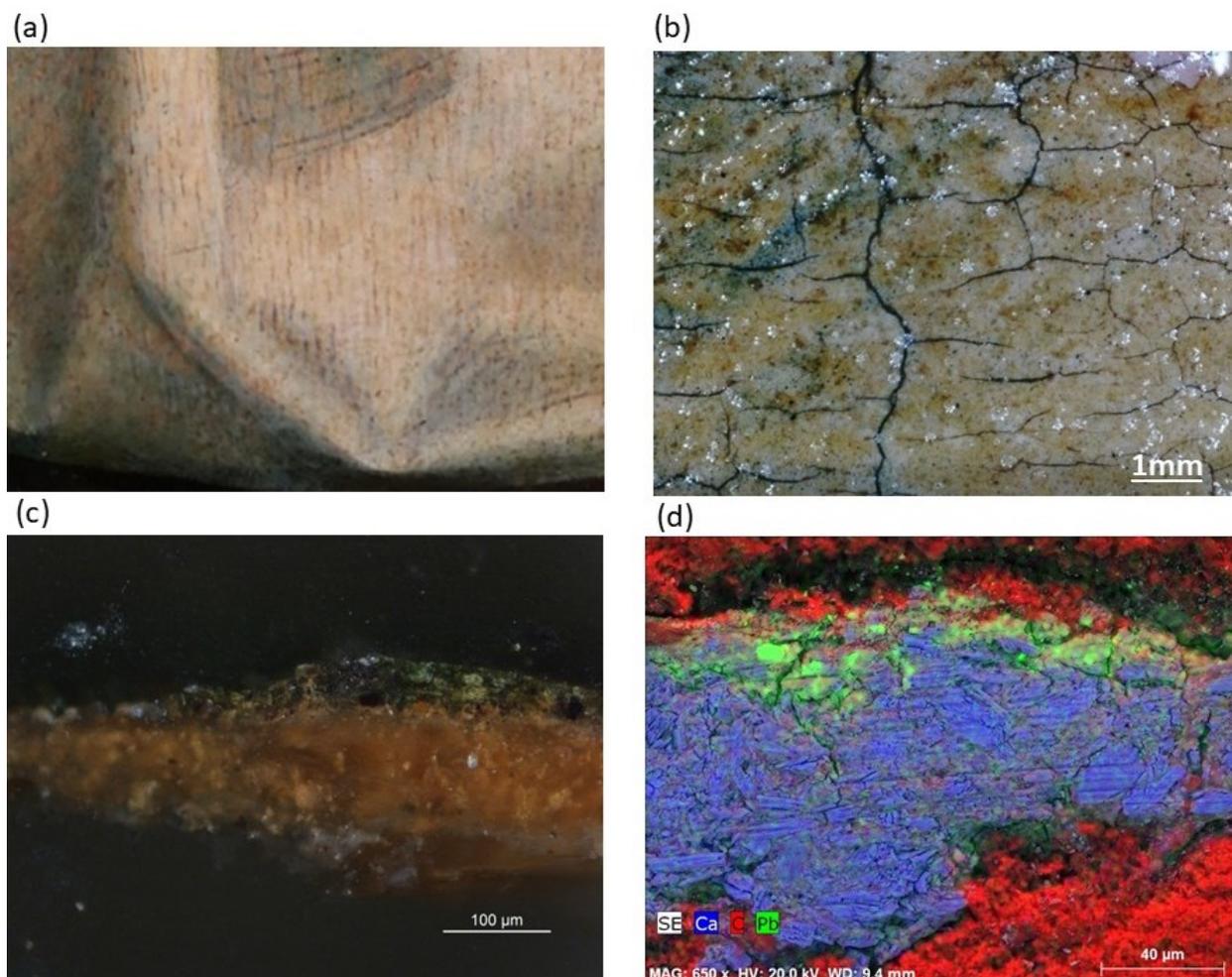
Figure 4. (**a**) Image of the underdrawings under the white vest of the angel; (**b**) macro-photography showing a closer look of the same aspect of the underdrawings; (**c**) sample P2-39 by OM, showing an undefined layer composed of red grains under the dark green layer; (**d**) the same sample under EDS mapping, confirming the presence of a Pb based underdrawing layer, probably minimum.

Three drawing stages are discernible.

1. An initial geometric layout establishing the placement of figures and architectural elements.
2. A refined contour drawing of the figures.
3. A final, fluid application of carbon-based medium with brush and pen, executed with great precision to faithfully replicate P1.

The portal decoration in P2 borrows motifs from Quentin Metsys's Water Wheel in front of Antwerp Cathedral—motifs Jorge Afonso likely knew through his brother-in-law, the Flemish painter Francisco Henriques, who worked in Portugal—while also introducing distinctive Portuguese details. A notable unfinished sketch of Queen D. Leonor's coat of arms adorns the front of P2, while the "525" inscription on the verso of P1—marking the year of her death—indicates that her passing likely prompted the commission of P2 and halted work on her arms [27]. On that same verso of P1, Jorge Afonso's signature appears above a profile sketch, highlighting P2's status as the inaugural panel before the fourteen-piece Setúbal altarpiece. Metsys himself signed and dated several of his panels—most famously the 1509 Triptyque de la confrérie de Sainte-Anne in Louvain's Saint Peter's Church [49]. Several profile sketches appear on the reverse of P2—similar to Jorge Afonso's profile under his signature in P1—and likely represent a late-life self-portrait (he died in

1540 at age 70) [27]. That very facial profile recurs among the Magi in his Adoração dos Magos panel for the Setúbal altarpiece and again in his Madre de Deus altarpiece in Lisbon (c. 1515), painted soon after his Sete Dores da Virgem series (1510–11) for the same convent (Figure 5).
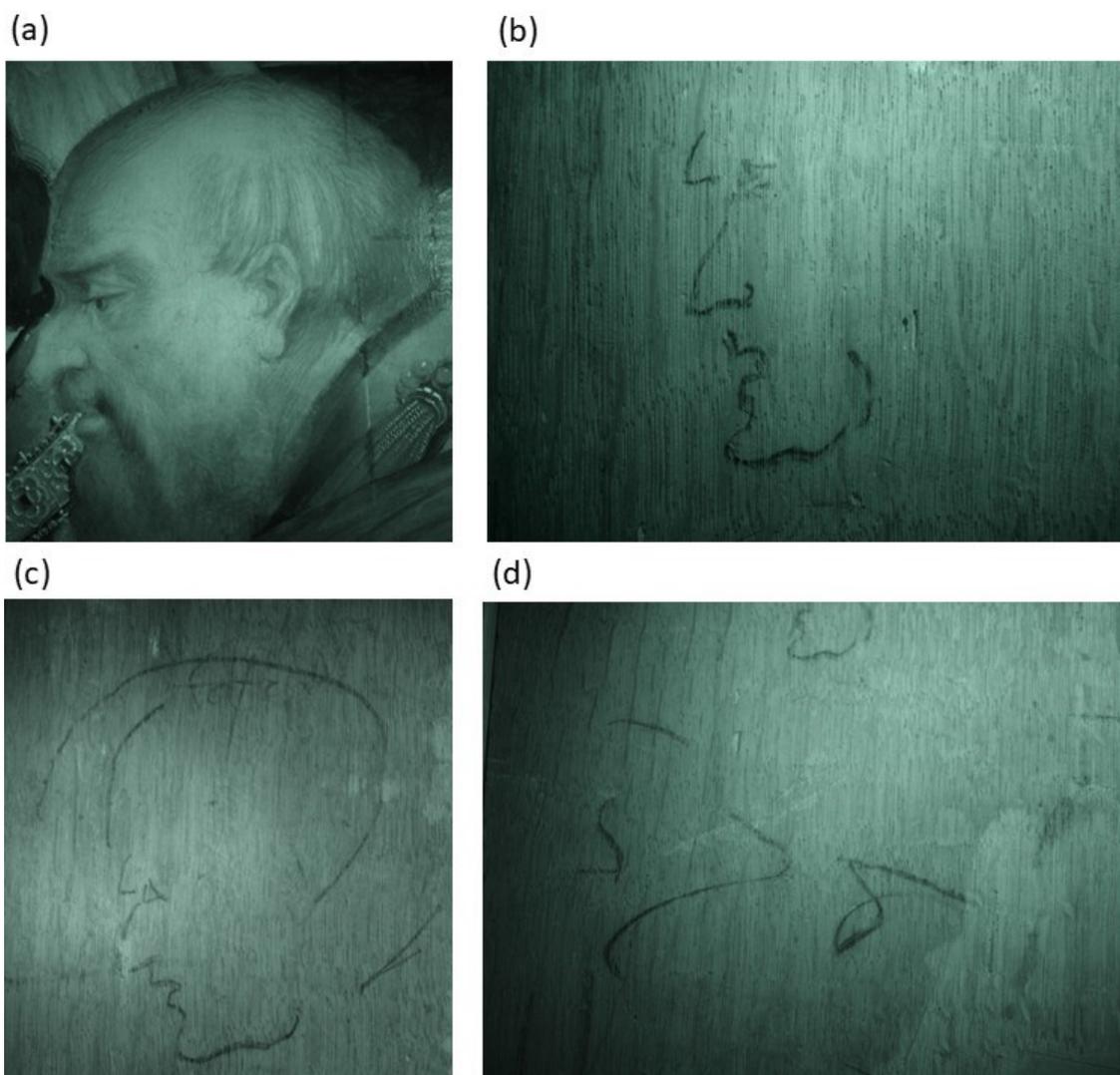

Figure 5. (**a**) Reflectogram of the underdrawings of the King Mage figure in the painting "Adoração dos Magos", the altarpiece of the church of the Convento de Jesus in Setúbal, Jorge Afonso, Portuguese school, 1525; (**b**) reflectogram detail of figure profile in the back of the painting "Apparition of the angel to Santa Clara, Santa Inês and Santa Coleta" (P1) assigned to Metsys workshop; (**c**) reflectogram detail of figure profile headed by Jorge Afonso signature in the back of P1 (**d**) date of 525 in the back of P1.

These final technical findings—and the parallel practices observed in both masters' workshops—underscore Quentin Metsys's profound influence on Jorge Afonso's early career, as long recognized in Portuguese art history. A master–apprentice connection between Metsys and Jorge Afonso has been suggested [16,18]. Moreover, Portuguese painters' ready access to the trade "feitorias" in Flanders—exemplified by Edward Portugalois, who served his apprenticeship in Metsys's workshop from 1504 to 1506—is attested in Damião de Góis's chronicle of King D. Manuel [50–52]. Further archival and technical research is required to confirm this hypothesis. At present, this study remains confined to these unique case studies, with additional documentary evidence still awaiting exploration [16].

3.4. Gold Leaf and Bolus

Gold-leaf application to the angel's wings and crown is unique to P1, whereas P2 employs gold only sparingly on the saints' halos. In P1, imitation-gold pigments are also used to render the monstrance—arguably the most cherished and intricately detailed element of the composition—likely to capture its minute ornamentation (Figure 6).
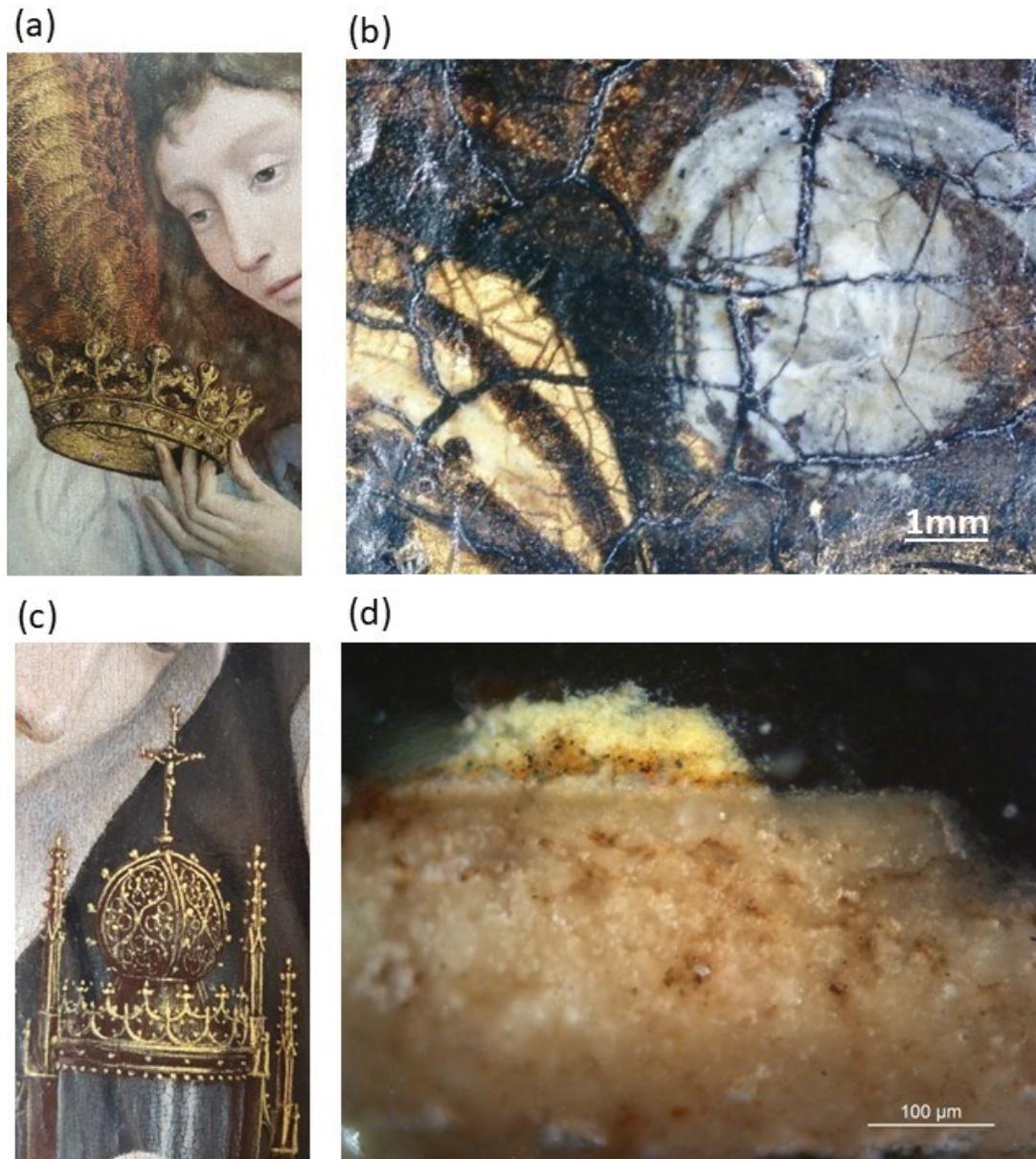

Figure 6. (**a**) Painting "Apparition of the angel to Santa Clara, Santa Inês and Santa Coleta" (detail from the crown), attributed to Quentin Metsys workshop, c. 1491–1507; (**b**) microphotography from the gold leaf under a pearl in the crown; (**c**) Monstrance from the same painting highlighting the minutes painted details imitating gold; (**d**) OM cross-section from sample P1-3, taken from the light area of the monstrance and highlighting the upper layer light tone, probably composed of lead-tin yellow.

The extensive use of gold leaf creates a pronounced contrast in both technique and intent between the two panels, reflecting a twenty-year shift from traditional to more modern workshop practices. In Antwerp, the master's workshop applied a bole layer followed by genuine gold leaf and then sealed it with translucent glazes to emphasize the principal symbols—the angel and the royal crown—whereas in Lisbon, Jorge Afonso's workshop

imitated gilded surfaces with pigmented mixtures, showcasing the painter's technical prowess in harmony with the anthropocentric ideals of Renaissance humanism [53].

In P1 (sample P1-7), XRF analysis of the angel's wing highlights revealed gold (Au), lead (Pb), copper (Cu), calcium (Ca), and iron (Fe). SEM-EDS imaging of the underlying bole layer confirmed the presence of lead, aluminum (Al), and silicon (Si) (Figure 2). Micro-Raman spectroscopy delineated a stratigraphy consisting of a lead-white ground, a vermilion bole, the gold leaf itself, and an overlying carbon-black layer (Table 1). μ-FTIR analysis of that bole layer detected kaolinite, cerussite, hydrocerussite, calcite, trace gypsum, quartz, drying oil, lead carboxylates and oxalates, all finished with a ketone-resin varnish—most likely Winsor and Newton's Artists' Retouching Varnish (Table 2).

In P1, XRF analysis of the angel's wing shadow (region P1-8) detected Au, Pb, Cu, Ca, and Fe. In the crown's gold leaf—examined in regions P1-35 (light tone) and P1-36 (shadow tone)—XRF revealed Au, Sn, Pb, Cu, Ca, and Fe. μ-Raman analysis of the underlying bole layer identified lead-tin yellow type I, plumbonacrite, calcite, hematite, cinnabar, and carbon black as its principal compounds (Table 1).

For the nimbus of St. Clara (region P1-14), XRF again showed Au and Pb. μ-Raman of the white layer there confirmed lead white and carbon black as the main constituents (Table 1). μ-FTIR of that bole layer further validated the presence of kaolinite, cerussite, hydrocerussite, calcite, trace gypsum, drying oil, protein, a ketone-resin varnish, and metallic carboxylates and oxalates (Table 2). The lavish application of gold leaf in architectural and figural elements was typical of Metsys's workshop—for instance, in The Virgin and Child Enthroned with Four Angels, Metsys adorns the architecture with genuine gold leaf [7].

By contrast, P2's "gilding" is entirely imitative. Pigment analysis shows a mixture of lead-tin yellow, lead white, ochre, and vermilion [19]. μ-FTIR of the saints' halos' bole layer reveals kaolinite, cerussite, hydrocerussite, quartz, drying oil, and lead carboxylates (Table 2).

3.5. Pigments and Layering

3.5.1. White Color

XRF analysis of region P1-1 reveals lead (Pb) in the white highlight of the angel's tunic. μ-Raman spectroscopy shows a calcite ground overlaid by a plumbonacrite layer ($Pb_{10}(CO_3)_6O(OH)_6$) with sparse hematite grains (Table 1). In region P1-2 (tunic shadow), XRF detects Pb and calcium (Ca), while μ-Raman identifies a red hematite layer surmounted by a black, azurite-rich layer used for shading (Table 1; Figure 6). μ-FTIR of the same stratigraphy reveals a pale blue layer—composed of azurite, cerussite, oil, and lead carboxylates—indicative of lead-white degradation (Table 2).

P2 exhibits a comparable palette: μ-FTIR of sample P2-2 detects a single pale blue layer containing azurite, cerussite, a ketone resin varnish, and metal carboxylates (Table 2). Unlike P1's multi-layer build-up, P2's white-shadow effects are achieved in a single application [19].

3.5.2. Yellow Color

XRF analysis of region P1-3—the yellow highlight on the monstrance—detected Pb, Ca, Fe, and Sn, and μ-Raman confirms this layer as lead-tin yellow type I (Pb_2SnO_4) mixed with carbon black (Table 1; Figure 7). Region P1-4 (the monstrance's shadow) likewise shows Pb, Ca, Fe, and Sn. In the ochre background's light tone (P1-5), XRF reveals Pb, Ca, and Fe, while the ochre shadow (P1-6) contains Pb, Ca, Fe, and Sn; μ-Raman identifies that the brown shadow layer as carbon black, hematite, and lead-tin yellow type I (Table 1).
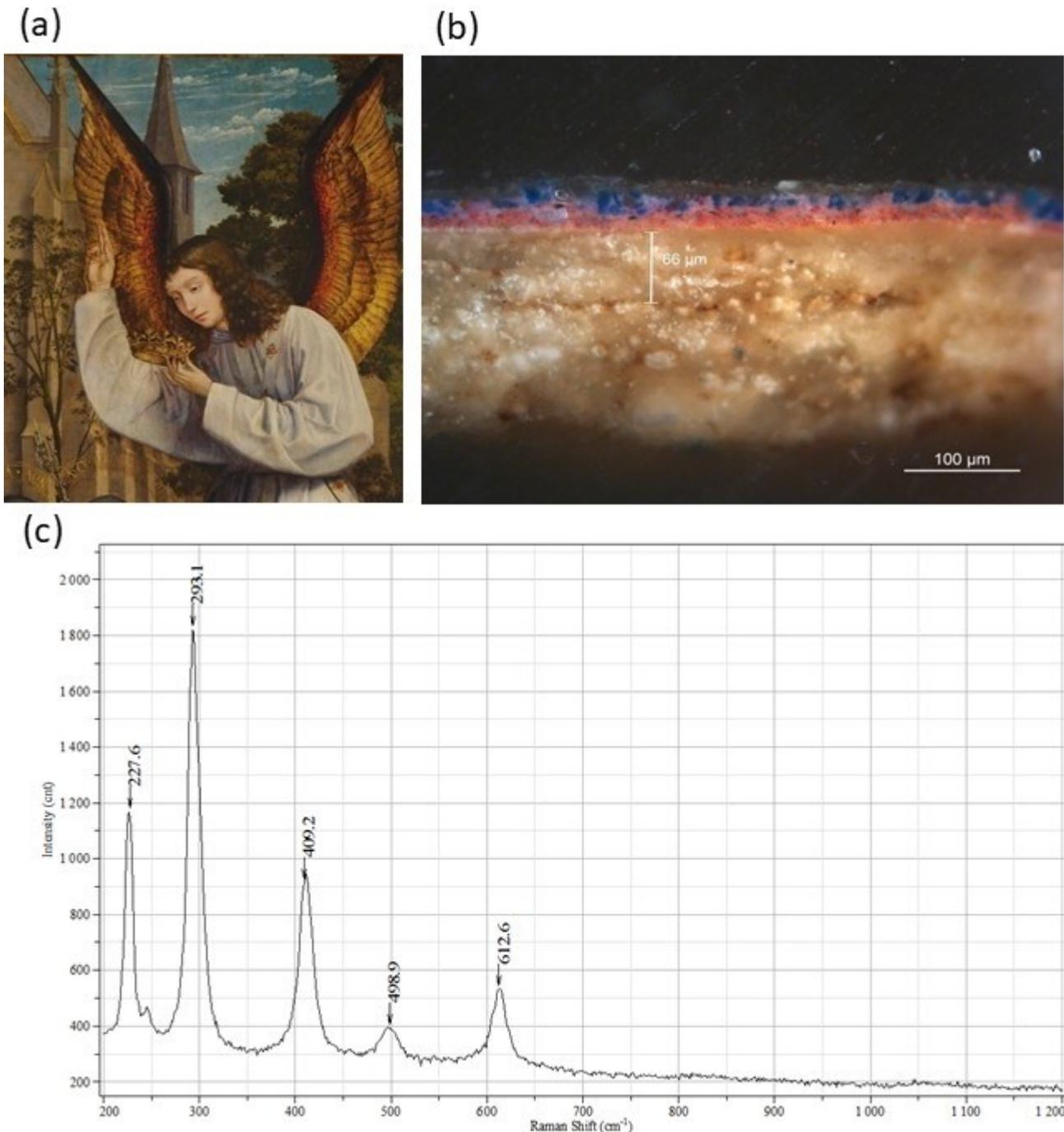
Figure 7. (**a**) Painting "Apparition of the angel to Santa Clara, Santa Inês and Santa Coleta" (detail), attributed to Quentin Metsys workshop, c. 1491–1507; (**b**) OM image of sample P1-2 taken from the white shadow vest of the angel, highlighting a first thin white priming layer, a second red layer and a third bluish layer/black layer; (**c**) hematite μ-Raman Spectrum highlighting peaks at 228, 293, 409, 499, and 613 cm^{-1} obtained at the red layer.

P2 displays an almost identical yellow palette—adding goethite, which was absent in P1—and, like P1, builds its yellow passages in two to three coats [19]. SEM-EDS mapping of sample P2-4 confirms a three-layer sequence: a Pb-rich base coat, an Fe-rich middle layer, and a Sn-bearing top layer, most likely lead-tin yellow (Figure 8).
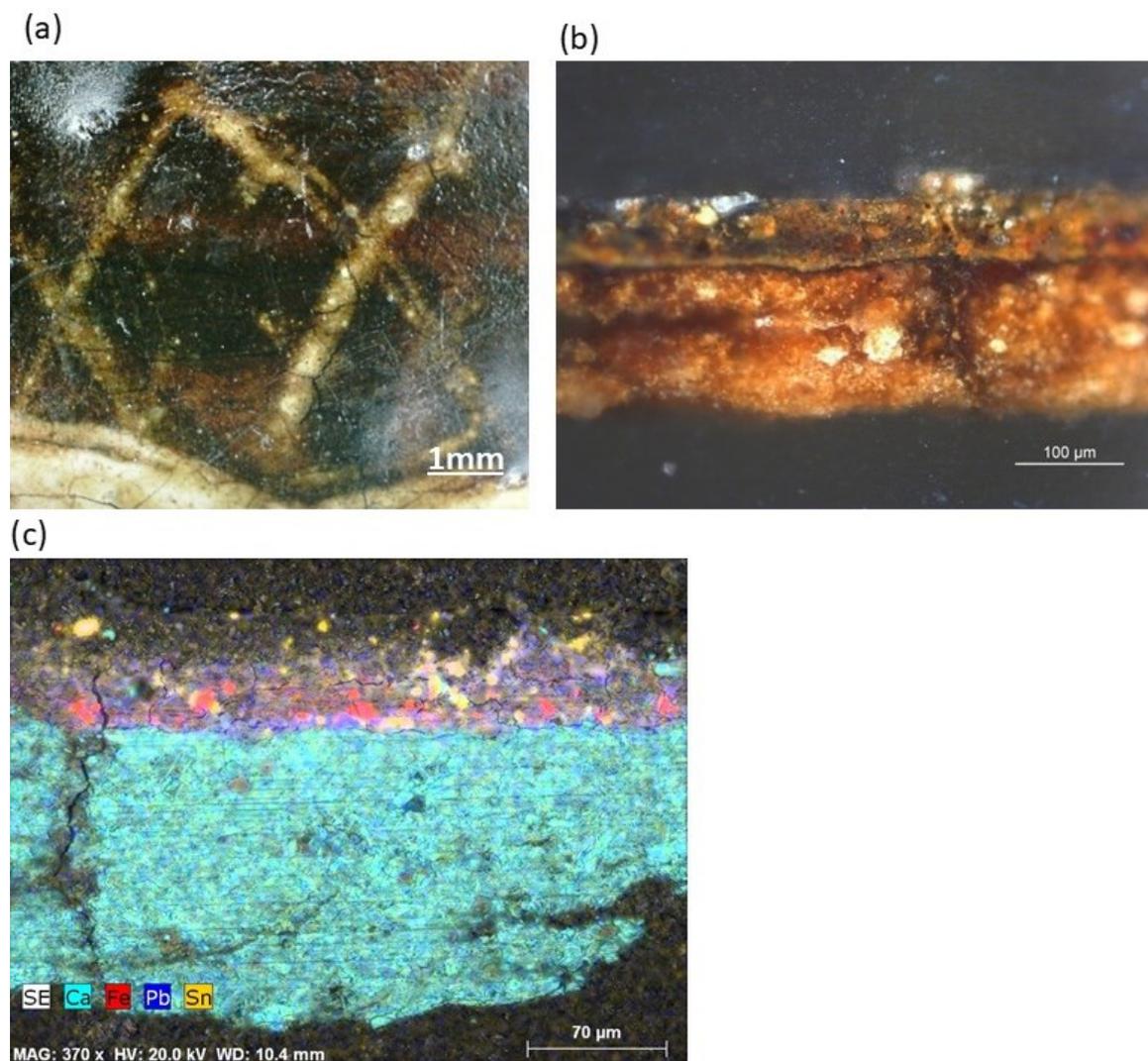
Figure 8. (**a**) Painting "Apparition of the angel to Santa Clara, Santa Inês and Santa Coleta" (P2) (monstrance detail), the altarpiece of the church of the Convento de Jesus in Setúbal, Jorge Afonso, Portuguese school, 1525; (**b**) OM cross-section image of sample PR2-4, taken from the brown shadow of the monstrance, showing a first thin black layer, a second light brown layer, and a third dark brown layer; (**c**) SEM-EDS mapping confirmed the presence of a first Pb-based layer, a second layer mainly composed by Fe and a third layer containing Sn, probably lead-tin yellow.

3.5.3. Red Color

Both panels employ essentially the same red pigments and stratigraphies—apart from P1's use of genuine gold leaf—and build their red passages in two to three successive layers [19].

Angel's Wing (P1-9): XRF of the red-light tone detects Au (from the gold leaf), Pb, Ca, and Fe. μ-FTIR further identifies a red lacquer layer containing cerussite, calcite, trace gypsum, silicates, and a ketone-resin varnish (Table 2).

Column (P1-11, P1-12): Micro-XRF of the column's light red tone (P1-11) and shadow (P1-12) reveals Pb, Ca, Fe, and Hg (Figure 9). μ-Raman confirms that the red layer is composed of hematite (Fe_2O_3) with a carbon-black admixture—underscoring hematite's role in the shadow passages (Table 1).

Apostle's Mantle (P1-13): XRF again shows Pb, Ca, Fe, and Hg in the red cloak. μ-Raman distinguishes a white underlayer of lead white and carbon black, topped by a thin cinnabar layer (Table 1; Figure 9).
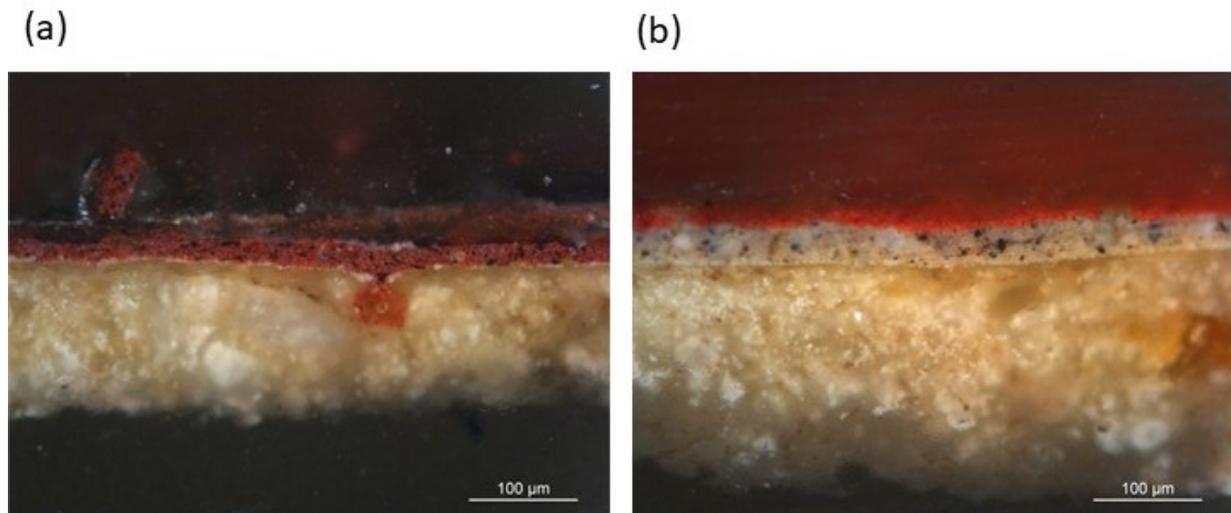
Figure 9. (**a**) OM cross-section image of sample P1-12, regarding the shadow tone of the column, showing a thin white priming layer under a red matrix layer; (**b**) OM cross-section image of sample P1-13, regarding the red mantle from the apostle, showing a thin white priming layer under a thick white matrix layer and a thin red layer.

3.5.4. Brown Color

Sta. Clara's Tunic (P1-15 and P1-16): XRF of the light-brown tunic (P1-15) and its shadow (P1-16) detected Pb, Ca, Fe, and Hg. μ-Raman confirms a brown paint layer composed of lead white, hematite, and carbon black (Table 1).

Architectural Elements (P1-17 and P1-18): In the light brown of the architecture (P1-17), XRF shows Pb, Cu, Ca, Fe, and Sn. μ-Raman identifies lead-tin yellow type I, lead white, and carbon black as the principal pigments. The shadow tone (P1-18) returns the same elemental signature (Table 1).

Angel's Hair (P1-19 and P1-20): XRF in both the light (P1-19) and shadow (P1-20) hair tones detects Pb, Cu, Ca, Fe, Hg, and Zn—the latter likely from a later repainting. μ-Raman reveals a layered system: a white underlayer of lead white, topped by brown vermilion (HgS), hematite, and carbon black (Table 1).

In P2, the same suite of brown pigments is present—but, unlike P1's multiple stratified coatings, P2 achieves its brown passages in a single, uniform layer [19].

3.5.5. Green Color

XRF of region P1-21 (light green ground) detects Sn, Pb, Cu, and Ca. μ-Raman identifies that layer as a mixture of lead-tin yellow type I, hematite, and carbon black (Table 1). In P1-22 (green floor shadow), XRF shows Fe, Pb, Cu, and Ca, while μ-Raman reveals carbon black and goethite as the principal compounds.

In the foliage (P1-23), XRF detects Cu, Fe, Pb, Ca, and Sn. Cross-sectional μ-Raman shows a three-stage build-up:

Lower "sky" layer of azurite ($Cu_3(CO_3)_2(OH)_2$) and cerussite ($PbCO_3$)

Intermediate gray modeling layer combining black and white (a technique characteristic of Metsys's workshop [7,54])

Upper green layer of plumbonacrite, lead-tin yellow type I, and malachite ($Cu_2CO_3(OH)_2$) (Figure 10; Table 1)

P1-24 (foliage shadow) yields the same XRF signature; μ-Raman again distinguishes a blue underlayer of azurite, cerussite, and hematite, with plumbonacrite indicating pigment degradation [55].

P2 mirrors these findings—identical elemental profiles and layering—except that malachite is absent. Instead, a final green glazed layer, likely verdigris, appears to have been applied [19] (Figure 10).
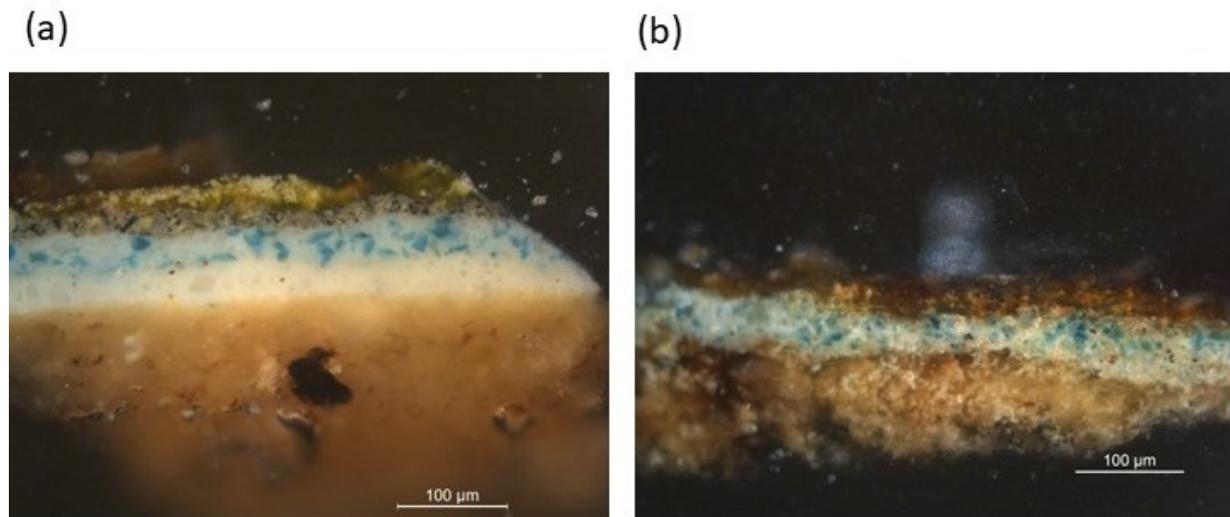

Figure 10. (**a**) OM cross-section image of sample P1-23, taken from the green light trees showing a thick white priming layer, the second layer in a blue matrix (sky), a third gray layer, a fourth green glazed layer (probably verdigris) and a fifth yellow layer corresponding to the light yellow traces; (**b**) OM cross-section image of sample PR2-24, taken from green shadow of the trees showing a thin white priming layer, the second layer in a blue matrix (sky), a third thin gray layer and a fourth green glazed layer (probably verdigris).

3.5.6. Blue Color

XRF analysis of region P1-25 (the sky's light blue tone) detected lead (Pb), copper (Cu), and calcium (Ca). Likewise, XRF of region P1-26 (the sky's shadow tone) revealed the same elements. μ-Raman spectroscopy confirms that these blue layers consist primarily of azurite, carbon black, lead white, and plumbonacrite—the latter likely a degradation product of lead white (Table 1).

In P2, elemental and molecular analyses largely mirror those of P1, with the addition of barite and a conspicuously thinner white priming layer beneath the blue paint [19] (Figure 10). This reduced priming thickness may result from applying the blue pigment directly onto a still-tacky ground, causing partial intermixing and a thinner overall preparatory coating.

3.5.7. Gray Color

In P1, XRF of the tower's light gray tone (region P1-27) detected iron (Fe), lead (Pb), and calcium (Ca). In the tower's shadowed gray (region P1-28), XRF revealed copper (Cu), Fe, Pb, Ca, and tin (Sn). μ-Raman analysis further indicates a bichromatic build-up: a basal layer of lead-tin yellow type I topped by a gray layer composed of carbon black, lead white, and azurite (Table 1).

3.5.8. Black Color

XRF analysis of P1-29 (the light black tone of Santa Clara's veil) detected Ca, Pb, Fe, Cu, and Sn; P1-30 (the veil's shadow) returned the same elemental profile. μ-Raman spectroscopy reveals a two-layer build-up: a yellow preparatory layer of lead-tin yellow type I, lead white, and carbon black, topped by a black paint layer of carbon black and red ochre as the principal pigments (Table 1). In the angel's wing (P1-10), XRF likewise shows Pb, Cu, Ca, and Fe, and μ-Raman confirms a single carbon-black layer. P2 displays

a virtually identical black-pigment palette [19]. μ-FTIR of sample P2-30 (Santa Clara's veil) identifies a black layer composed of cerussite, quartz, gypsum, ketone resin, oil, and metallic carboxylates (Table 2).

3.5.9. Flesh Tone

XRF of region P1-31 (the light flesh tone on Sta. Clara's hand) detected Ca, Hg, Pb, Fe, and Cu. μ-Raman spectroscopy shows this passage to consist of a flesh-toned organic layer, lead-tin yellow type II, and lead white. In region P1-32 (the hand's shadow tone), XRF revealed Ca, Hg, and Pb, and μ-Raman identified a mixture of carbon black and lead white.

Optical microscopy of cross-section P1-33 (the angel's hand, light flesh tone) uncovers a thin pink paint layer atop a thicker white preparatory layer (Figure 11). XRF analyses of both P1-33 and its corresponding shadow (P1-34) detected Hg, Pb, Cu, Fe, and Ca in each. μ-Raman confirms that these layers comprise carbon black, lead white, hematite, and cinnabar (Table 1).
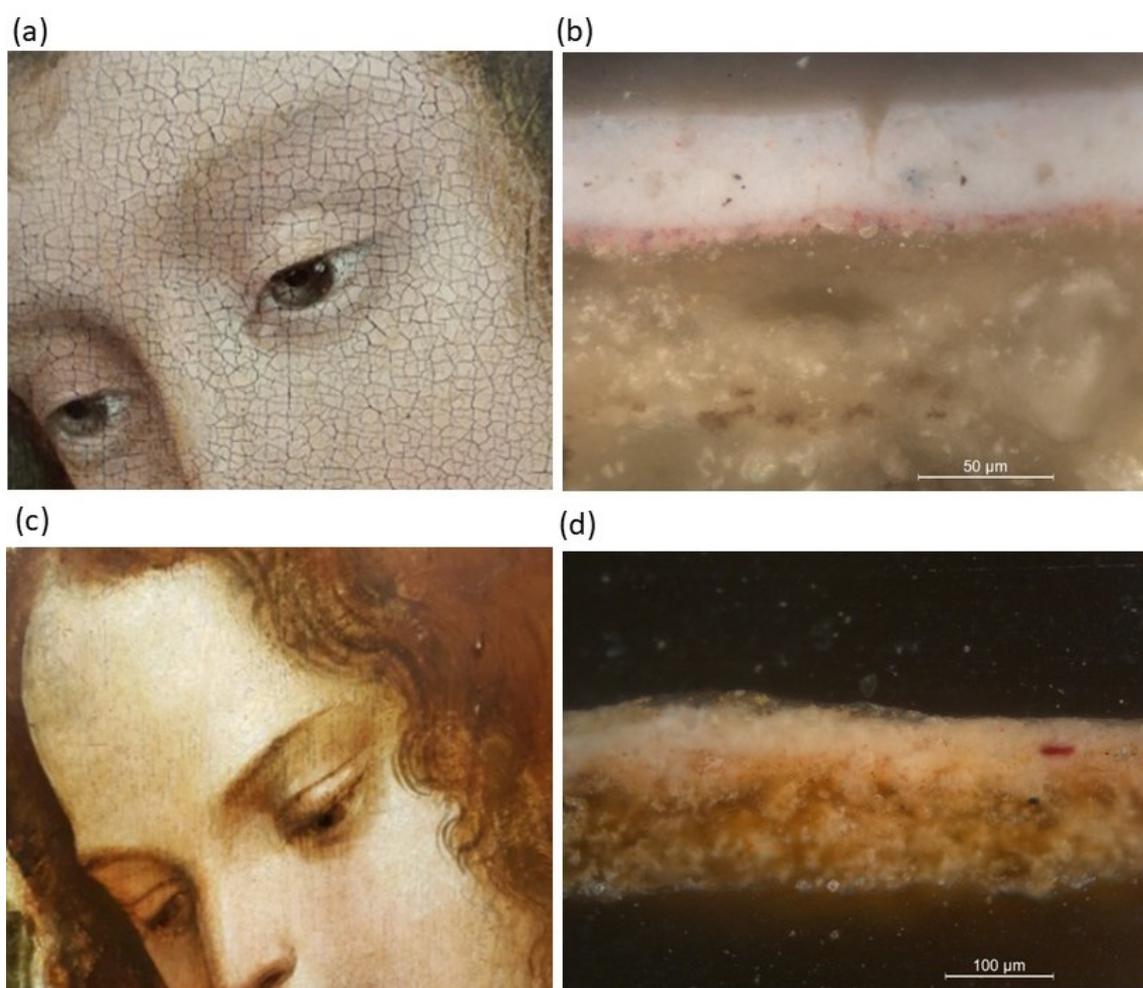

Figure 11. (**a**) Painting "Apparition of the angel to Santa Clara, Santa Inês and Santa Coleta"(P1) (detail), attributed to Quentin Metsys workshop, c. 1491-1507; (**b**) OM cross-section of sample P1-33, taken from the light tone from the angel's hand, evidence a thin pink layer under a thicker white layer; (**c**) painting "Apparition of the angel to Santa Clara, Santa Inês and Santa Coleta"(P2) (detail), the altarpiece of the church of the Convent of Jesus of Setúbal, Jorge Afonso, Portuguese school, 1525; (**d**) OM cross-section of sample P2-33, taken from the shadow tone from the angel's hand, evidence a pink layer under a white layer containing an organic red lacquer (red dot).

SEM-EDS mapping of P1 (Figure 12) reveals a thin, iron-rich pink paint layer resting above a thicker, whitish preparatory layer high in lead white. In P2, the elemental and

molecular composition is essentially the same, but the stratigraphy comprises two mixed coats: a deeper, darker pink base layer overlain by a lighter pink layer containing lead white, vermilion, bone black, lead-tin yellow, and an organic red dye [19].
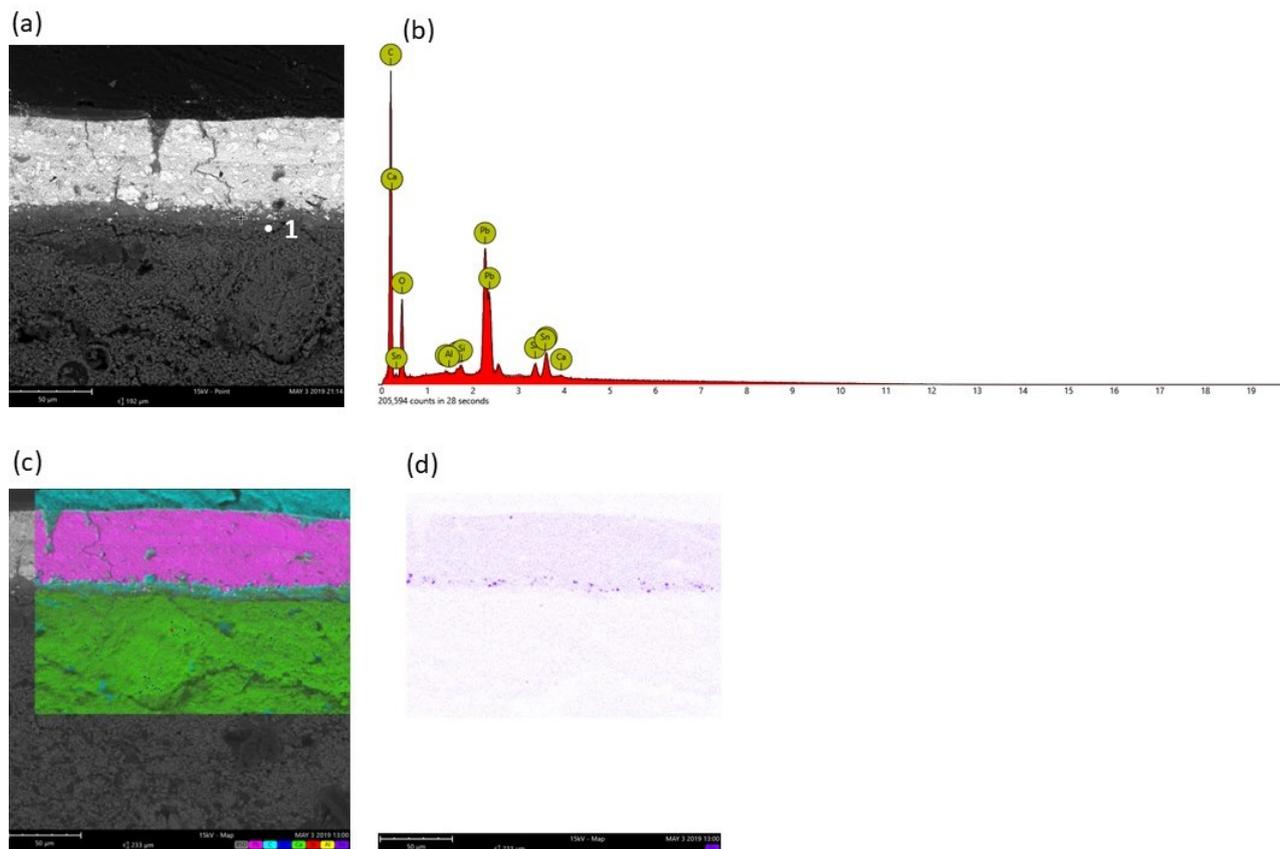

Figure 12. (**a**) SEM (BSE) image of sample P1-33 highlighting the presence of coccoliths and foraminifera fossils, in the ground layer and marks the point "1" where EDS analysis was performed; (**b**) SEM-EDS spectrum of elements found in "1": a carbon-rich layer, being identified also Ca, Pb, Sn, Al, and Si; (**c**) SEM-EDS mapping for P1-33 sample reveals a thinner carbon-based and Fe-rich pink layer under a thicker whitish layer containing these last elements a bigger quantity of Pb (lead white); (**d**) SEM-EDS map of Fe element, highlighting the Fe-rich thin layer.

Micro-FTIR analysis of sample P2-32 (the shadowed flesh tone on Sta. Clara's hand) identifies a black layer composed of cerussite, gypsum, quartz, wax, ketone resin, drying oil, and lead carboxylates (Table 2). Optical microscopy of cross-section P2-33 (the angel's hand shadow) shows a thin pink paint layer over a white ground that includes an organic red lacquer (Figure 11).

4. Conclusions

The results of this study demonstrate that, while Jorge Afonso adopted certain Flemish conventions, his workshop's choice of materials and methods remained fundamentally rooted in Southern European practice.

First, both panels share practical similarities—most notably the use of Baltic oak for their supports and a two-stage ground system with progressively thinner top coats. Yet, their compositions diverge: the Northern workshop employed chalk (calcium carbonate) throughout its multilayered ground, whereas Jorge Afonso's workshop chose an anhydrite-rich calcium sulfate matrix, reserving only minor carbonate additions in the uppermost layer to refine its surface.

Gold leaf provides another clear point of departure. P1's extensive gilt—on the angel's wings and crown—reflects the Antwerp workshop's preference for natural gold and bole, glazed to accentuate key iconography. In P2, gold is confined to saintly halos, with most "gilded" effects rendered in pigments. This shift—from materials supplied by nature to effects achieved by the artist—mirrors a broader, humanist turn in early sixteenth-century taste [48].

Both painters applied an average of three paint layers per color and drew from almost identical palettes. However, Jorge Afonso's pigments were less finely ground, resulting in subtle intermixing at layer boundaries, whereas the Flemish workshop maintained crisp stratigraphic separations.

Most strikingly, their underdrawing practices reveal contrasting workshop cultures. P1's draftsmanship is almost invisible under infrared reflectography, limited to sparse, low-carbon marks or pattern-transfer techniques, consistent with a high-volume studio output. In P2, drawing is paramount: a precise, multistage carbon sketch—with abandoned corrections—extends even to the panel's verso, where Jorge Afonso boldly inscribed his signature above a profile study. Here, the underdrawing becomes both a creative record and an assertion of authorship. In elevating his own hand—literally positioning himself atop a collaborative medium—Jorge Afonso stakes his claim as the great master and true founder of the Lisbon school, emulating the prestigious status that Metsys had already achieved in Antwerp.

Author Contributions: Conceptualization, V.A.; Formal analysis, S.V., A.C. (Ana Cardoso), A.L. and M.M.; Investigation, A.C. (Ana Cardoso) and M.L.C.; Resources, A.C. (António Candeias), J.M. and M.J.F.; Writing—original draft, V.A.; Writing—review & editing, M.L.C. All authors have read and agreed to the published version of the manuscript.

Data Availability Statement: Data is contained within the article.

Conflicts of Interest: The authors declare no conflict of interest.

Notes

[1] The Portuguese feitoria in Flanders was an official Crown-sanctioned trading post, initially established in Bruges and later relocated to Antwerp during the 15th and 16th centuries. It served as a structured node within Portugal's overseas commercial network, facilitating trade in goods such as spices, sugar, and wine, and ensuring diplomatic and fiscal coordination with the merchant economies of Northern Europe.

References

1. Nichols, J.G. XXVIII.—Remarks on some Pictures of Quintin Matsys and Holbein, in the Collection of the Earl of Radnor, at Longford Castle. *Archaeologia* **1874**, *44*, 435–458. [CrossRef]

2. Jongen, L.; Boëllet, N. Wanneer het God behaagt, Voortgang. Neerlandistiek VU Foundation, Amsterdam. *Progress* **2009**, *27*, 26–45.

3. Filedt Kok, J.P.; Bruijnen, Y.; Bikker, J. Early Netherlandish paintings in the Rijksmuseum, Amsterdam. Artists born before 1500. *Bus. Strategy Environ.* **2009**, *1*.

4. Woodall, J. De wisselaer: Quentin Matsys's Man weighing gold coins and his wife. *Neth. Yearb. Hist. Art/Ned. Kunsthist. Jaarb. Online* **2014**, *63*, 38–75. [CrossRef]

5. Born, A.; Martens, M. O políptico de Quinten de Metsys para o convento da Madere de Deus: Notas sobre a técnica. In *Casa Perfeitíssima: 500 anos da Fundação do Mosteiro da Madre de Deus, Museu Nacional do Azulejo, Ministério da Cultura*; Curvelo, A., Ed.; Instituto dos Museus e da Conservação: Lisboa, Portugal, 2009; pp. 155–166.

6. Carvalho, J.A.S. 159–Tríptico do Baptismo de Cristo. In *Cristo Fonte de Esperança*; Porto, D.d., Azevedo, C.A.M., Eds.; Diocese do Porto: Porto, Portugal, 2000; pp. 260–261.

7. Dunkerton, J. The Technique and Restoration of 'The Virgin and Child Enthroned, with Four Angels' by Quinten Massys. *Natl. Gallery Tech. Bull.* **2008**, *29*, 60–75.

8. Hirsch, E.F. Damião de Gois and the Arts. In *Damião de Gois*; Archives Internationales d'Histoire des Idees/International Archives of the Historry of Ideas: The Hague, The Netherlands, 1967; Volume 19.

9. Fouto, C. Damião de Góis's Livro de Linhagens: An Untold (Hi)story. *Port. Stud.* **2015**, *31*, 235–249. [CrossRef]

10. Lorena, M. A pintura flamenga em Portugal–os retábulos de Metsys, Morrison e Ancede. In *Estudo Técnico e Material*; Universidade de Évora, Museologia: Évora, Portugal, 2013.

11. Lorena, M. Altarpiece painting: A view from the inside. *E-Conserv. J.* **2015**, *3*, 118–138.

12. Cruz, A.J. Ser Ou Não Ser Metsys: O Desenho Subjacente Do Tríptico Da Vida De Cristo, De Tomar, e a Sua Atribuição Autoral. *Artis Rev. História Arte Ciências Património* **2017**, *5*, 104–113.

13. Eires, E.A.F. O tríptico da vida de Cristo, estudo e Tratamento de Pintura Sobre Madeira da Igreja de São João Baptista, em Tomar, atribuída à oficina de Quentin Metsys. Doctoral Dissertation, IPT-Instituto Politécnico de Tomar, Tomar, Portugal, 2015.

14. Cruz, A.J.; Eires, E.; Dias, L.; Desterro, T.; Rego, C. Identification of vivianite, an unusual blue pigment, in a sixteenth-century painting and its implications. *Colour Res. Appl.* **2018**, *43*, 177–183. [CrossRef]

15. Pereira, F.A.B.; Batoréo, M.; Alves, A.N.; Jesus, A.; Francisco, M.J. *Retábulo do Convento de Jesus de Setúbal*; Câmara Municipal de Setúbal: Setúbal, Portugal, 2013.

16. Caetano, J.O. Jorge Afonso, uma Interrogação Essencial na Pintura Primitiva Portuguesa. Doctoral Dissertation, Universidade de Évora, Museologia, Évora, Portugal, 2013.

17. Reis-Santos, L. Jorge Afonso, coi. In *Nova Colecção de Arte Portuguesa*; Artis: Lisboa, Portugal, 1966.

18. Flor, P. Notas sobre Jorge Afonso e o Mestre da Charola de Tomar. Artis, revista do Instituto de História da arte da Faculdade de Letras da Universidade de Lisboa. *Sep. Da Rev. Artis–Rev. Do Inst. De História Da Arte Da Fac. De Let. De Lisb.* **2009**, *7*, 73–78.

19. Antunes, V.; Candeias, A.; Valadas, S. Travelling masterpieces from Flanders to Portugal: Jorge Afonso's Portuguese "copy" of Quentin Metsys's "Apparition of the Angel to Saints Clare, Agnes, and Colette". In *Art, Travel, and Exchange Between Iberia and Global Geographies, c.1400-1550*; Beltrami, C., Alvares-Correa, S., Eds.; Brill: Leiden, The Netherlands, 2025; pp. 384–404, Chapter 12.

20. Guerra, M.; Manso, M.; Longelin, S.; Pessanha, S.; Carvalho, M.L. Carvalho, Performance of three different Si X-ray detectors for portable XRF spectrometers in cultural heritage applications. *J. Instrum. 14th Int. Workshop Radiat. Imaging Detect. (IWORID2012)* **2012**, *7*, C10004.

21. Guerra, M.; Manso, M.; Pessanha, S.; Longelin, S.; Carvalho, M.L. Theoretical and Experimental Study on the Angular Dependence of Scattering Processes in XRF Systems. *X-Ray Spectrom.* **2013**, *42*, 402–407. [CrossRef]

22. Bell, I.M.; Clark, R.J.; Gibbs, P.J. Raman spectroscopic library of natural and synthetic pigments (pre- $\approx$ 1850 AD). *Spectrochim. Acta Part A Mol. Biomol. Spectrosc.* **1997**, *53*, 2159–2179. [CrossRef] [PubMed]

23. Burgio, L.; Clark, R.J.H. Library of FT-Raman spectra of pigments, minerals, pigment media and varnishes, and supplement to the existing library of Raman spectra of pigments with visible excitation. *Spectrochim. Acta Part A Mol. Biomol. Spectrosc.* **2001**, *57*, 1491–1521. [CrossRef]

24. Downs, R.T. The RRUFF Project: An integrated study of the chemistry, crystallography, Raman, and infrared spectroscopy of minerals. In Proceedings of the Program and Abstracts of the 19th General Meeting of the International Mineralogical Association, Kobe, Japan, 23–28 July 2006; p. 117.

25. Brewer, P.W.; Murphy, D.; Jansma, E. TRiCYCLE: A universal conversion tool for digital tree-ring data. *Tree-Ring Res.* **2011**, *67*, 135–144. [CrossRef]

26. Rinn, F. *TSAP-Win User Reference Manual*; Rinntech: Heidelberg, Germany, 2010.

27. Antunes, V.; Candeias, A.; Mirão, J.; Carvalho, M.L.; Dias, C.B.; Manhita, A.; Cardoso, A.; Francisco, M.J.; Lauw, A.; Manso, M. Analytical characterization of the palette and painting techniques of Jorge Afonso, the great 16th century Master of Lisbon painting workshop. *Spectrochim. Acta. Part A Mol. Biomol. Spectrosc.* **2017**, *193*, 264–275. [CrossRef]

28. Billinge, R.; Campbell, L.; Dunkerton, J.; Foister, S.; Kirby, J.; Pilc, J.; White, R. Methods and Materials of Northern European Painting in the National Gallery, 1400–1550. *Natl. Gallery Tech. Bull.* **1997**, *18*, 6–55.

29. Roy, A.; Smith, P.; Bomford, D. *Painting Techniques, History, Materials and Studio Practice: Contributions to the Dublin Congress, 7–11 September 1998*; International Institute for Conservation of Historic and Artistic Works: London, UK, 1998.

30. Antunes, V.; Candeias, A.; Coroado, J.; Serrão, V.; Cachão, M.; Carvalho, M.L. A multidisciplinary approach to the study of the brightening effects of white chalk ground layers in 15th and 16th century paintings. *Anal. Methods* **2016**, *8*, 4785–4797. [CrossRef]

31. Klein, P. Dendrochronological analyses of Netherlandish panel paintings. In *La Pintura Europea Sobre Tabla. Siglos XV, XVI y XVII*; Ministerio de Cultura: Madrid, Spain, 2010; pp. 94–99. Available online: https://dialnet.unirioja.es/servlet/articulo?codigo=40 86462 (accessed on 13 May 2025).

32. Vandivere, A.L.S. *From the Ground Up: Surface and Sub-Surface Effects in Fifteenth-and Sixteenth-Century Netherlandish Paintings*; Faculty of Humanities, Instituut voor Cultuur en Geschiedenis: Spinhuis: Amsterdam, The Netherlands, 2013.

33. Antunes, V.; Oliveira, M.J.; Vargas, H.; Serrão, V.; Candeias, A.; Carvalho, M.L.; Coroado, J.; Mirão, J.; Dias, L.; Longelin, S.; et al. Characterization of glue sizing under calcium carbonate ground layers in flemish and luso-flemish painting-analysis by SEM-EDS, μ-XRD and μ-Raman. *Anal. Methods* **2014**, *6*, 710–717. [CrossRef]

34. Davies, M. Early Flemish Painting. By Margaret Whinney. 10 × 7½. Pp. 168 + 100 pls. London: Faber & Faber, 1968. 70s. *Antiqu. J.* **1969**, *49*, 168–169.

35. Antunes, V. Techniques and Materials of Preparation in the Portuguese Painting of the XV and XVI Centuries. Doctoral Dissertation, Universidade de Lisboa, História, Portugal, 2014.

36. Antunes, V.; Candeias, A.; Oliveira, M.J.; Lorena, M.; Seruya, A.I.; Carvalho, M.L.; Gil, M.; Mirao, J.; Coroado, J.; Gomes, V.; et al. Calcium sulphate fillers and binders in Portuguese 15th and 16th centuries: Ground layers from a family painting workshop-Study by multianalytical spectroscopic techniques. *Microchem. J.* **2016**, *125*, 290–298. [CrossRef]

37. Antunes, V.; Candeias, A.; Mirão, J.; Carvalho, M.L.; Serrão, V.; Dias, C.B.; Manhita, A.; Cardoso, A.; Manso, M. On the origin of Goa Cathedral former altarpiece: Material and technical assessment to the work of Garcia Fernandes, Portuguese painter from 16th century Lisbon workshop. *Microchem. J.* **2018**, *138*, 226–237. [CrossRef]

38. Antunes, V.; Candeias, A.; Mirão, J.; Serrão, V.; Dias, C.B.; Manhita, A.; Cardoso, A.; Manso, M.; Carvalho, M.L. A Painter in the Shadow: Unveiling Conservation, Materials and Techniques of the Unknown Luso-Flemish Master of Lourinhã. *Heritage* **2019**, *4*, 2725–2744. [CrossRef]

39. Antunes, V.; Candeias, A.; Oliveira, M.J.; Carvalho, M.L.; Dias, C.B.; Manhita, A.; Francisco, M.J.; Costa, S.; Lauw, A.; Manso, M. Uncover the mantle: Rediscovering Gregorio Lopes palette and technique with a study on the painting "Mater Misericordiae". *Appl. Phys. A-Mater. Sci. Process.* **2016**, *122*, 1–14. [CrossRef]

40. Antunes, V.; Candeias, A.; Oliveira, M.J.; Longelin, S.; Serrão, V.; Seruya, A.I.; Coroado, J.; Dias, L.; Mirao, J.; Carvalho, M.L. Characterization of gypsum and anhydrite ground layers in 15th and 16th centuries Portuguese paintings by Raman Spectroscopy and other techniques. *J. Raman Spectrosc.* **2014**, *45*, 1026–1033. [CrossRef]

41. Valadas, S.; Freire, R.V.; Cardoso, A.; Mirão, J.; Dias, C.B.; Vandenabeele, P.; Candeias, A. On the Use of the Unusual Green Pigment Brochantite ($Cu_4(OH)_6(SO_4)$) in the 16th-Century Portuguese-Flemish Paintings Attributed to The Master Frei Carlos Workshop. *Microsc. Microanal.* **2015**, *21*, 518–525. [CrossRef] [PubMed]

42. Morrison, E.; Kren, T. *Flemish Manuscript Painting in Context: Recent Research*; Getty Trust Publications: J. Paul Getty Museum Series; J. Paul Getty Museum: Los Angeles, CA, USA, 2007; p. 208, ISBN 9780892368525.

43. Bomford, D.; Billinge, R.; Campbell, L.; Dunkerton, J.; Foister, S.; Kirby, J.; Plazzotta, C.; Roy, A.; Spring, M. *Art in the Making: Underdrawings in Renaissance Paintings*; National Gallery: Londres, UK, 2002.

44. Thompson, D.V. *The Materials and Techniques of Medieval Painting*; Dover Publications: Nova Iorque, NY, USA, 1936.

45. Cennini, C.; Thompson, D.V. The craftsman's handbook. In *The Italian "Il libro dell' arte."*; Thompson, D.V., Translator; Dover Publications: New York, NY, USA, 1960.

46. Duval, A.; Guicharnaud, H.; Dran, J.-C. Particle induced X-ray emission: A valuable tool for the analysis of metalpoint drawings. *Nucl. Instrum. Methods Phys. Res. Sect. B Beam Interact. Mater. At.* **2004**, *226*, 60–74. [CrossRef]

47. Watrous, J. *The Craft of Old-Master Drawings*; University of Wisconsin Press: Madison, IN, USA, 1957.

48. Merrifield, M.P. *Original Treatises, Dating from the XIIth to the XVIIIth Centuries, on the Arts of Painting: In Oil, Miniature, Mosaic, and on Glass; of Gilding, Dyeing, and the Preparation of Colours and Artificial Gems; Preceded by a General Introduction; with Translations, Prefaces, and Notes*; Merrifield, Ed.; John Murray: Albemarle, NC, USA, 1849; Volume 2.

49. Even, E.V.; Metsys, Q. *Notice Biographique sur le Peintre Quinten Matsys de Louvain*; Louvain University: Louvain, Belgium, 1846.

50. Santos, L.R.; Portugalois, E.; Novais, M. *Eduardo, o Português*; Artis: Lisboa, Portugal, 1966.

51. Puyvelde, L.V. *Edouard Portugalois*; Bruckmann: München, Germany, 1960.

52. Goes, D.D. *Cronica do Felicissimo rei D. Manuel*; Imprensa da Universidade: Coimbra, Portugal, 1926.

53. Stoichita, V.I. *La Invención del Cuadro: Arte, Artífices y Artificios en Los Orígenes de la Pintura Europea*; Ediciones Cátedra: Madrid, Spain, 2011.

54. Vandivere, A. "Cloeck en veerdigh": Energetic and Skillful Painting Techniques of the Sixteenth-Century Leiden School. *J. Hist. Netherlandish Art* **2012**, *4*, 1. [CrossRef]

55. Cotte, M.; Checroun, E.; Nolf, W.D.; Taniguchi, Y.; Viguerie, L.D.; Burghammer, M.; Walter, P.; Rivard, C.; Salomé, M.; Janssens, K.; et al. Lead soaps in paintings: Friends or foes? *Stud. Conserv.* **2017**, *62*, 2–23. [CrossRef]